Condensation transitions in a two-species zero-range process

T. Hanney and M. R. Evans
School of Physics, University of Edinburgh, Mayfield Road, Edinburgh EH9 3JZ, United Kingdom
(Received 14 August 2003; published 22 January 2004)

We study condensation transitions in the steady state of a zero-range process with two species of particles. The steady state is exactly soluble—it is given by a factorized form provided the dynamics satisfy certain constraints—and we exploit this to derive the phase diagram for a quite general choice of dynamics. This phase diagram contains a variety of mechanisms of condensate formation, and a phase in which the condensate of one of the particle species is sustained by a ''weak'' condensate of particles of the other species. We also demonstrate how a single particle of one of the species (which plays the role of a defect particle) can induce Bose condensation above a critical density of particles of the other species.

DOI: 10.1103/PhysRevE.69.016107 PACS number(s): 05.70.Fh, 02.50.Ey, 64.60.−i

I. INTRODUCTION

Condensation phenomena are observed in a variety of contexts. For instance, microscopic dynamics including particle diffusion, aggregation to form particle clusters, and fragmentation of these clusters can be used to model a number of physical systems [1,2]. In one dimension, such models have been analyzed within mean field theory [1] or using a scaling approach [2] to infer the existence of transitions between a fluid phase and a condensate phase. Another context is the modeling of granular and traffic flow [3]. One such model is the ''Bus Route model'' [4], where there is a crossover between a regime in which the average velocity of buses is determined by the velocity of the slowest bus, and, above a critical density of buses, a regime in which the average bus velocity is limited instead by the high density of traffic. This crossover can be understood in terms of a condensation process. Further, several models have been shown to undergo phase separation in one dimension [5,6]. This phase separation can also be related to a condensation mechanism. In particular, a general criterion has been proposed, predicting the existence of phase separation in 1-*d* driven systems, which appears to be widely applicable [7]. This applicability follows from the robust nature of the physical mechanism underlying the phase separation. This mechanism, which is also the generic mechanism for the aforementioned condensation phenomena, is understood in terms of condensation transitions in the zero-range process [8].

The zero-range process is a system of many interacting particles which move on a lattice—particles hop to adjacent lattice sites with hop rates determined by the number of particles present at the departure site. It provides insight into the behavior of more complicated models because it is exactly soluble: the steady state assumes a simple, factorized form. This factorized form holds for an arbitrary lattice in any dimension, although for simplicity the one-dimensional model in usually considered. Thus the condensation transitions, whereby a finite fraction of particles occupy a single site, are amenable to exact analysis. Condensation transitions in the single-species zero-range process proceed through one of two mechanisms: (i) if the particle hop rates are site dependent, then above a critical density a condensate forms at the site where the hop rate is slowest—this mechanism is closely related to Bose condensation, (ii) if the particle hop rates depend on the number of particles present at the departure site, then above a critical density, and provided the asymptotic dependence decays to a constant value sufficiently quickly, a condensate forms at a site located at random—thus the transition is accompanied by a spontaneously broken symmetry. The former mechanism here demonstrates how disorder can induce condensation, analysis of the latter leads to an understanding of the generic mechanism of condensate formation applicable to the examples described above.

A question which naturally arises then is what other generic mechanisms of condensate formation exist. To this end, we consider the generalization of the zero-range process to two species of particles. We investigate how the interaction of the two species allows a variety of mechanisms of condensate formation.

The zero-range process with two species of particles was introduced in Refs. [9,10] where the steady state was obtained exactly and shown to be given by a simple factorized form provided the dynamics satisfy certain constraints. In Ref. [9], this was used to demonstrate a new mechanism of condensation transition for a specific choice of dynamics, and in [10] the hydrodynamics were derived. Here, we show how the two-species model may undergo a wide variety of condensation transitions, and we derive the phase diagram for the model for a quite general choice of dynamics. Also, we show that the steady state of the model can be mapped onto the steady state of the Arndt-Heinzel-Rittenberg (AHR) model [5]—a model which undergoes a transition between a disordered (fluid) phase and a phase separated (condensate) phase. Thus, as in the single-species model, the two-species zero-range process exhibits transitions of a robust nature which can provide insight into condensation mechanisms in more complicated models. In particular, one perspective of the two-species model is to consider one species as providing an evolving landscape upon which the other species in turn evolves. This evolution is coupled, thus condensation transitions are induced by the evolving disordered background. Again, such interplay arises in a variety of physical settings [11–13]. Our aim is to explore how this interplay can lead to

condensation transitions in the two-species zero-range process.

We begin by reviewing in Sec. II the key equations of the steady state solution, which form the basis of the subsequent analysis. In Sec. III, we show how a defect particle (i.e., a single particle of one of the species) can induce a condensation transition in the particles of the other species. We consider in Sec. IV the case where the hop rates of one of the particle species depend only on the number of particles of the other species at the departure site. We show how to derive the phase diagram for this case and find that three distinct condensate phases can arise; numerical iterations of an exact recursion relation for the partition function yield results consistent with the predicted phases. In Sec. V we present a mapping between the steady state of the two-species zero-range process and the AHR model. We conclude in Sec. VI.

II. STEADY STATE

We define the two-species zero-range process on a lattice containing L sites and with periodic boundary conditions. On this lattice, there are N particles of species A and M particles of species B. Particles of both species hop to the nearest neighbor site to the right, species A with rate $u(n_l,m_l)$ and species B with rate $v(n_l,m_l)$, where site l is the departure site and contains n_l particles of species A and m_l particles of species B. Although we consider a one-dimensional lattice, the factorized steady state holds for a hypercubic lattice in any dimension. Therefore all the phase transitions that follow also hold in any dimension.

Since the steady state has already been derived in detail elsewhere [9,10], we quote only the key results here. We define $P(\{n_l\};\{m_l\})$ to be the probability of finding the system in the configuration $(\{n_l\};\{m_l\})$, where $\{n_l\}=n_1,\ldots,n_L$ and $\{m_l\}=m_1,\ldots,m_L$. This is given by a factorized form

$$P(\{n_l\};\{m_l\})=Z_{L,N,M}^{-1}\prod_{l=1}^{L} f(n_l,m_l), \tag{1}$$

where $Z_{L,N,M}$ is a normalization. The steady state (1) satisfies the steady state master equation if the factors $f(n_l,m_l)$ satisfy

$$\frac{u(n_l,m_l)f(n_l,m_l)}{f(n_l-1,m_l)}=1 \quad \text{and} \quad \frac{v(n_l,m_l)f(n_l,m_l)}{f(n_l,m_l-1)}=1. \tag{2}$$

The solution to these equations is

$$f(n_l,m_l)=\prod_{i=1}^{n_l}[u(i,m_l)]^{-1}\prod_{j=1}^{m_l}[v(0,j)]^{-1}, \tag{3}$$

provided the hop rates satisfy the constraint

$$\frac{u(n_l,m_l)}{u(n_l,m_l-1)}=\frac{v(n_l,m_l)}{v(n_l-1,m_l)}, \tag{4}$$

for $n_l,m_l\neq 0$—the choices of $u(n_l,0)$ and $v(0,m_l)$ remain unconstrained. We emphasize that instead of specifying the hop rates directly, we have the freedom to choose any desired form for $f(n,m)$ and that we can then infer the hop rates from Eq. (2).

The normalization $Z_{L,N,M}$, defined in Eq. (1), plays a role analogous to the canonical partition function of equilibrium statistical mechanics, and is given by

$$Z_{L,N,M}=\sum_{\{n_l\},\{m_l\}}\delta\left(\sum_{l=1}^{L}n_l-N\right)\delta\left(\sum_{l=1}^{L}m_l-M\right)\times\prod_{l=1}^{L}f(n_l,m_l), \tag{5}$$

where the δ-functions ensure that the system contains the correct numbers of particles of each species. By writing the δ-functions in an integral representation, $Z_{L,N,M}$ becomes

$$Z_{L,N,M}=\oint\frac{dz}{2\pi i}\oint\frac{dy}{2\pi i}\frac{[F(z,y)]^L}{z^{N+1}y^{M+1}}, \tag{6}$$

where the generating function $F(z,y)$ has been defined as

$$F(z,y)=\sum_{n=0}^{\infty}\sum_{m=0}^{\infty}z^n y^m f(n,m). \tag{7}$$

We consider in Sec. IV the limit $L,N,M\to\infty$, where $\rho_A=N/L$ and $\rho_B=M/L$—the particle densities of species A and B, respectively—are held fixed. In this limit, we assume that the integral in Eq. (6) is dominated by the saddle point. The equations for the saddle point are

$$\rho_A=z\frac{\partial}{\partial z}\ln F(z,y), \quad \rho_B=y\frac{\partial}{\partial y}\ln F(z,y). \tag{8}$$

Assuming the saddle point is valid, Eqs. (8) determine ρ_A and ρ_B in terms of z and y and this amounts to working in a grand canonical ensemble. We note that for the saddle point to be valid, z and y cannot exceed the radii of convergence of $F(z,y)$, since we must be able to perform the sum (7) in the first place. Further, since all derivatives of $F(z,y)$ are positive, the saddle point, if valid, must be unique. In Sec. IV we will find that it is not always possible to solve the saddle point equations for all values of ρ_A and ρ_B in the allowed ranges of z and y. This phenomenon corresponds to a condensation transition.

III. DEFECT PARTICLE

In this section, we consider how condensation may arise when there is only a single particle of species B. The hop rates of the A particles are chosen to be

$$u(n,0)=1 \quad \text{and} \quad u(n,1)=p, \tag{9}$$

where $p<1$, such that the A particles hop more slowly when the B particle is present (but they hop independently of n).

Thus we view the B particle as a defect particle. The constraint on the hop rates (4) then requires that the hop rate of the B particle is

$$v(n,0)=0 \quad \text{and} \quad v(n,1)=p^n. \tag{10}$$

Substituting these dynamics into Eq. (3), one finds that $f(n,0)=1$ and $f(n,1)=p^{-n}$. For this model, we can evaluate Eq. (5) as a finite sum (i.e., we can work directly in the canonical ensemble). Taking the B particle to be at site k one obtains

$$Z_{L,N,M}=L\sum_{\{n_l\}}\delta\left(\sum_{l=1}^{L} n_l-N\right)p^{-n_k} \tag{11}$$

$$=L\sum_{n_k=0}^{N}\binom{L-2+N-n_k}{L-2}p^{-n_k}. \tag{12}$$

This is the same normalization (up to an overall factor of L) as that derived for the single-species model with heterogeneous hop rates, in the case where particles hop from all sites with rate 1 except for a single defect site from which particles hop with rate p [8]. Thus, using the results of Ref. [3], one can identify two regimes: a low density phase, when $\rho_A<p/(1-p)$, and the system is in a fluid phase; and a high density phase, when $\rho_A>p/(1-p)$, and a Bose condensate forms at the site containing the defect particle. These regimes can be computed exactly by considering the normalization (12), and seeing that the sum may be dominated either by $n_k\sim O(1)$, in which case $\rho_A<p/(1-p)$, or by $n_k\sim O(L)$, in which case $\rho_A>p/(1-p)$ [8]. The condensate then contains a finite fraction of all the particles in the system—the remaining particles form a power law distributed background. It is a Bose condensate in the sense that the particles condense onto the site containing the defect particle (in the same way that in Bose condensation, the particles condense into the state of lowest energy: the equivalence is observed by identifying the site containing the defect particle in the zero-range process with the state of lowest energy in the Bose gas).

A condensation transition of this kind persists as long as we have a finite number of (indistinguishable) defect particles: let us say there are M defect particles where in the limit $L\to\infty$, we keep M fixed. Also, the hop rates for the A particles are $u(n,m)=p_m$ where $m=1,\ldots,M$. If the smallest of these hop rates is p_i, then above a critical density of A particles, all the sites containing i particles of species B contain a finite fraction of all the particles of species A. But because there can only be a finite number of such sites, each of these sites must contain an infinite number of particles of species A—the condensate is distributed equally among the sites containing i particles of species B.

The analysis of this section leads us to view the defect particle(s) as a disordered background upon which A particles evolve. The special feature of the two-species model is that this background may also evolve with prescribed dynamics. This is the case we consider in the following section, when the number of B particles is extensive.

IV. FINITE DENSITIES OF BOTH SPECIES

With the perspective of particle dynamics on an evolving disordered background, a case of particular interest in the two-species zero-range process is when the evolution of one species, the B particles say, depends only on the number of particles of the other species at a site. Therefore we take $v(n,m)=1+r(n)$ for $m>0$, where $r(n)$ is a general function of n. Then from Eq. (2) we deduce that $f(n,m)$ is given by

$$f(n,m)=[1+r(n)]^{-m}s(n), \tag{13}$$

where $s(n)$ is another general function of n. We then use Eq. (2) to infer the rates $u(n,m)$:

$$u(n,m)=\left(\frac{1+r(n-1)}{1+r(n)}\right)^{-m}\frac{s(n-1)}{s(n)}. \tag{14}$$

We assume in the following that $r(n)$ is a monotonically decreasing function of n, and that in the limit $n\to\infty$, $r(n)\to 0^+$. Inserting the form (13) into Eq. (7), and performing the sum over m, yields

$$F(z,y)=\sum_{n=0}^{\infty} s(n)z^n\frac{1+r(n)}{1+r(n)-y}, \tag{15}$$

$$z\frac{\partial}{\partial z}F(z,y)=\sum_{n=0}^{\infty} ns(n)z^n\frac{1+r(n)}{1+r(n)-y}, \tag{16}$$

$$y\frac{\partial}{\partial y}F(z,y)=\sum_{n=0}^{\infty} s(n)z^n\frac{y[1+r(n)]}{[1+r(n)-y]^2}. \tag{17}$$

These equations determine z and y, given the densities ρ_A and ρ_B, via Eq. (8). The radius of convergence of the sum over m is $y=1$ and we take, without loss of generality, the radius convergence of the sum over n to be $z=1$.

To analyze the possible transitions, we need to elucidate the behavior of ρ_A and ρ_B when considered as a function of z and y. This will enable us to draw graphs of the dependences of ρ_A and ρ_B on y, for fixed values of z, from which we can determine the densities for which the saddle point approximation remains valid. In particular, we wish to consider how ρ_A and ρ_B change as z and y approach their radii of convergence—if ρ_A or ρ_B tends towards a finite value, then condensation ensues. To this end, we make the following observations.

(1) For fixed z, ρ_A and ρ_B are monotonically increasing functions of y.

(2) For $z\to 0$, $\rho_A\to 0$.

(3) For $y\to 0$, $\rho_B\to 0$.

(4) For $z<1$, ρ_B is finite for all y (including $y=1$).

We supplement these observations with the following three conditions on $r(n)$ and $s(n)$, which determine whether ρ_A and ρ_B converge to finite or infinite values when z and y approach their radii of convergence. For $z\to 1$ and $y<1$, if, as $n\to\infty$,

$$ns(n)\to 0 \quad \text{faster than } 1/n, \tag{18}$$

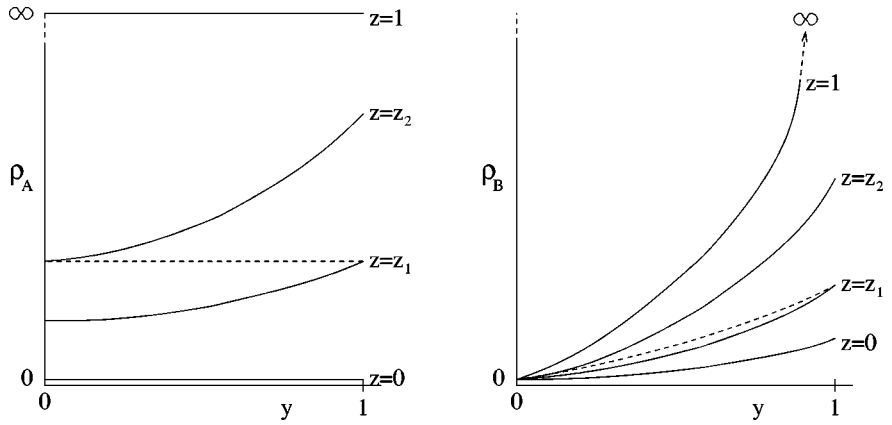

FIG. 1. Schematic dependences, for $b<2$, of the particle densities ρ_A and ρ_B for contours of fixed z and as a function of y. The dashed line in the right-hand graph illustrates how ρ_B varies as a function of z and y given that ρ_A is fixed (dashed line in left-hand graph).

then $\rho_A \to$ finite. For $z \to 1$ and $y \to 1$, if, as $n \to \infty$,

$$\frac{ns(n)}{r(n)} \to 0 \quad \text{faster than } 1/n, \tag{19}$$

then $\rho_A \to$ finite. For $z \to 1$ and $y \to 1$, if, as $n \to \infty$,

$$\frac{s(n)}{r(n)^2} \to 0 \quad \text{faster than } 1/n, \tag{20}$$

then $\rho_B \to$ finite. These observations and conditions enumerate all possible ways that z and y approach their radii of convergence, and therefore all the possible circumstances in which condensation can occur in our model. The phase behavior depends on which of the conditions (18)–(20) are met and which are not.

There are several possibilities, which we illustrate for a particular choice of $r(n)$ and $s(n)$, namely, for large n,

$$s(n) \sim n^{-b}, \quad r(n) \sim cn^{-1}, \tag{21}$$

where b and $c>0$ are constants. Thus the asymptotic forms of the hop rates for large n are given by

$$u(n,m) \sim (1-c/n^2)^m(1+b/n) \quad \text{and} \quad v(n,m) \sim 1+c/n. \tag{22}$$

We note that when $c=0$ the two species hop independently; in this case, the asymptotic hop rates of the A particles reduce to those considered in Ref. [8] for the single-species zero-range process, where condensation was found above a critical density provided $b>2$.

With the choice (21), condition (18) is satisfied if $b>2$ and conditions (19) and (20) are satisfied if $b>3$. Therefore there are three cases to consider.

Case 1: $b<2$. In this case, none of the conditions (18)–(20) is met. The particular choice of rates studied in Ref. [9] corresponds to this case. The dependences of ρ_A and ρ_B on y for fixed values of z are shown in Fig. 1, where $0<z_1<z_2<1$. Here, for a given ρ_A, z must lie in the range $z_1 \leqslant z \leqslant z_2$. However, in this range, ρ_B increases monotonically from $\rho_B=0$, where $y=0$ and $z=z_2$, to a maximum value at $y=1$ and $z=z_1$. If ρ_B exceeds this maximum then we can no longer solve the saddle point equations (8) for both ρ_A and ρ_B and the excess B particles condense onto a single site. Therefore whenever ρ_B exceeds a ρ_A-dependent maximum, the system is in a condensate phase. Otherwise the system is in a fluid phase. The critical line, given as a function of z for $y=1$, is shown in Fig. 2. The explicit expression for the critical line is

$$\rho_B = (1+\rho_A)/c. \tag{23}$$

The condensate of B particles [which contains $O(L)$ particles] is induced by the distribution of A particles. In particular, at the site containing the B particle condensate, the A particles form a "weak" condensate [which contains $O(L^{1/2})$ particles]. To see this, note that the current of A particles must be finite, therefore $u(n,m)$ must be finite at the condensate site. With the rates inferred from Eq. (21), if $m \to \infty$ then $u(n,m) \to 0$ unless we also have $n \to \infty$. Therefore taking n large one finds that $u(n,m) \sim \exp(-m/n^2)$. Since this must be finite we must have $m \sim n^2$ at the condensate site. Then, because $m \sim O(L)$, we must have $n \sim O(L^{1/2})$. Away from the condensate site, the B particles form a power law distributed background and the A particles form an exponentially distributed background.

We can understand the weak condensate of A particles by considering a zero-range process with a single defect site.

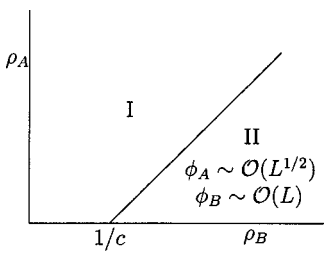

FIG. 2. Phase diagram for case 1, $b<2$. Phase I is a fluid phase; in phase II the B particles form a condensate sustained by a "weak" condensate of A particles, as described in the text. ϕ_A and ϕ_B denote the numbers of particles contained in the condensates of A and B particles, respectively.

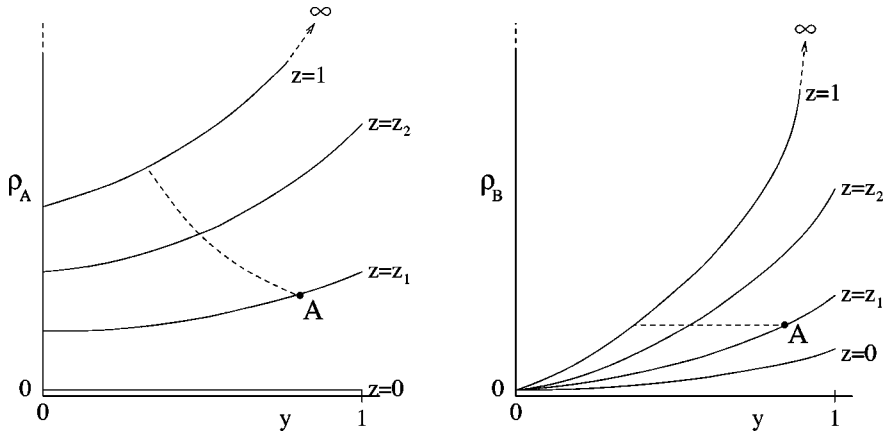

FIG. 3. Schematic dependences, for $2<b<3$, of the particle densities ρ_A and ρ_B for contours of fixed z and as a function of y. See text for details.

Consider a single species of particles—the A particles—which hop with rate $u(n)=1$ except at the defect site, where they hop with rate $u(n)=\exp(-gL/n^2)$ (g is a constant). The hop rate from the defect site reflects the effect of the B particle condensate on the A particles in the two-species model. At the defect site, $u(n)\to 0$ if n is small and so a condensate forms. But since the hop rate must remain finite, the condensate contains $n\sim O(L^{1/2})$ particles. Hence, from the perspective of the A particles, the condensate of B particles in the two-species model plays the role of a defect site.

Case 2: $2<b<3$. In this case, only condition (18) is met: ρ_A is finite for $z=1$ provided $y<1$. In this case, the dependences of ρ_A and ρ_B on y for fixed values of z are shown in Fig. 3, again where $0<z_1<z_2<1$. This time, imagine that the system is in the fluid phase, with densities ρ_A and ρ_B (and therefore values of z and y) corresponding to point A in Fig. 3. Now, if we add more A particles to the system while keeping the density of B particles fixed, we find that we must increase z and decrease y as indicated by the dashed line. However, when z reaches 1, if we add more A particles to the system we can no longer solve the saddle point equations for z and y, therefore the A particles must undergo a transition from a fluid phase to a condensate phase. The critical line is given by $z=1$—the critical density of A particles increases with increasing ρ_B. We have not been able to find an explicit expression for this critical line. Also note that at $y=1$, the system must undergo a transition between a fluid phase and a condensate of B particles as described in the previous case. Thus we deduce the phase diagram shown in Fig. 4. The two critical curves intersect when $\rho_A=\infty$ and $\rho_B=\infty$. In phase III, the condensate of A particles exists on a power law distributed background of A particles while the B particles are exponentially distributed throughout the system. It is interesting to consider the sequence of transitions induced by increasing ρ_B: starting from a point in phase III, the condensate of A particles is destroyed by increasing the density of B particles sufficiently, when the system enters the fluid phase I. Increasing ρ_B further leads the system to phase II where the B particles condense.

Case 3: $b>3$. Here, all the conditions (18)–(20) are satisfied. The arguments of the previous two cases apply but now, the critical curves given by $z=1$ on the one hand and $y=1$ on the other intersect at finite values of both ρ_A and ρ_B. Therefore when the A and B particle densities exceed their values given by $z=1$ and $y=1$ the system enters a phase where both species form a condensate at the same site. In this phase, the background distributions of A and B particles are both given by power laws. The phase diagram for this case is shown in Fig. 5.

We have confirmed the existence of the four phases presented in this section numerically. Exact expressions for $P(n)$, the probability of finding exactly n A particles at a site, and $P(m)$, the probability of finding exactly m B particles at a site, can be obtained in terms of the normalization $Z_{L,N,M}$. This normalization satisfies an exact recursion equation [9]

$$Z_{L,N,M}=\sum_{n=0}^{N}\sum_{m=0}^{M} f(n,m)Z_{L-1,N-n,M-m}, \qquad (24)$$

which is easily obtained from Eq. (5), and which can be iterated on a computer. Doing so, for systems up to size $L=100$ with $b=4$ and $c=2$, yields the distributions shown in Fig. 6. Four phases are evident. The circles represent densities $\rho_A=1/2=\rho_B$ and both species are in a fluid phase (phase I). The crosses represent densities $\rho_A=1/2$ and $\rho_B=3$, and

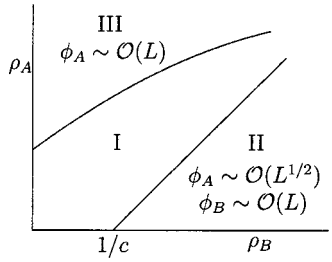

FIG. 4. Phase diagram for case 2, $2<b<3$. Phase I is a fluid phase; in phase II the B particles form a condensate sustained by a "weak" condensate of A particles, as described in the text. A condensate of A particles and fluid of B particles form in phase III. ϕ_A and ϕ_B denote the numbers of particles contained in the condensates of A and B particles, respectively.

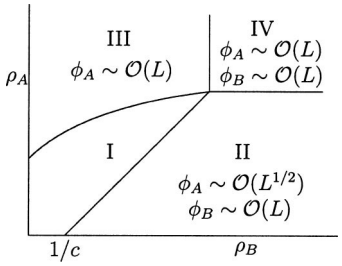

FIG. 5. Phase diagram for case 3, $b>3$. In region I both species are in a fluid phase; in region II the B particles are in a condensate phase sustained by a weak condensate of A particles; in region III the A particles are in a condensate phase and the B particles form a fluid; in region IV both species are in a condensate phase. ϕ_A and ϕ_B denote the numbers of particles contained in the condensates of A and B particles, respectively.

the distributions are consistent with a condensate of B particles on a power law distributed background, and a "weak" condensate of A particles containing $n \sim O(L^{1/2})$ particles, on an exponentially distributed background (phase II). The diamonds represent densities $\rho_A=3$ and $\rho_B=1/2$ and the A particles form a condensate on a power law distributed background, while the B particles form a fluid (phase III). The squares represent densities $\rho_A=7/2$ and $\rho_B=7/2$ and both species form condensates on power law distributed backgrounds (phase IV).

It is possible to generalize the choice for $r(n)$ in Eq. (21) to, for example, $r(n) \sim c n^{-d}$ where $d>0$ is a constant. This does not lead to any phase diagrams topologically distinct from those already presented, although it does lead to the possibility of ρ_B converging to a finite value as $\rho_A \to \infty$, and vice versa, as z and $y \to 1$. Thus the phase diagrams in Figs. 2 and 4 may be modified such that the phase boundaries tend toward a finite value of ρ_B as $\rho_A \to \infty$, and vice versa also in the case of Fig. 4. Another feature of this generalized choice for $r(n)$ is that in the phase II, where the B particles condense, the accompanying weak condensate of A particles contains a number of particles $n \sim O(L^{1/(1+d)})$, as may be verified using the argument expressed in case 1.

V. RELATION TO THE AHR MODEL

In this section, we show that steady state of the two-species zero-range process has a mapping on to the steady state of the AHR model.

The AHR model, introduced in Ref. [5], is a generalization of the second-class particle system studied in Ref. [15]. It is defined on a ring of $L+N+M$ sites, on which there are N + particles, M − particles, and L vacancies (which we represent by 0's). The dynamics are defined by the processes

$$\begin{aligned} +0 &\to 0+ \quad \text{with rate } \beta, \\ 0- &\to -0 \quad \text{with rate } \alpha, \\ +- &\to -+ \quad \text{with rate } 1, \\ -+ &\to +- \quad \text{with rate } q, \end{aligned} \tag{25}$$

where each exchange takes place between nearest neighbor sites. For $\alpha=\beta=1$ the model undergoes a transition between a disordered phase ($q<1$) and a phase separated phase ($q>1$) composed of a single domain of each species. The correspondence between the AHR model and the two-species zero-range process may be observed in the following way.

We define $w(\{\tau_i\})$ to be the steady state weight for the system to be in a configuration $\{\tau_i\}=\tau_1, \ldots, \tau_{L+N+M}$. The weights $w(\{\tau_i\})$ can be obtained using a matrix ansatz [5,14,15], that is, we write the particle configuration as a product of matrices

$$\{\tau_i\} = X_1 \cdots X_{L+N+M}, \tag{26}$$

where the matrix X_i is

$$X_i = \begin{cases} D & \text{if } \tau_i = + \\ E & \text{if } \tau_i = - \\ A & \text{if } \tau_i = 0. \end{cases}$$

Then it can be shown that the steady state weights can be written in the form [14,15]

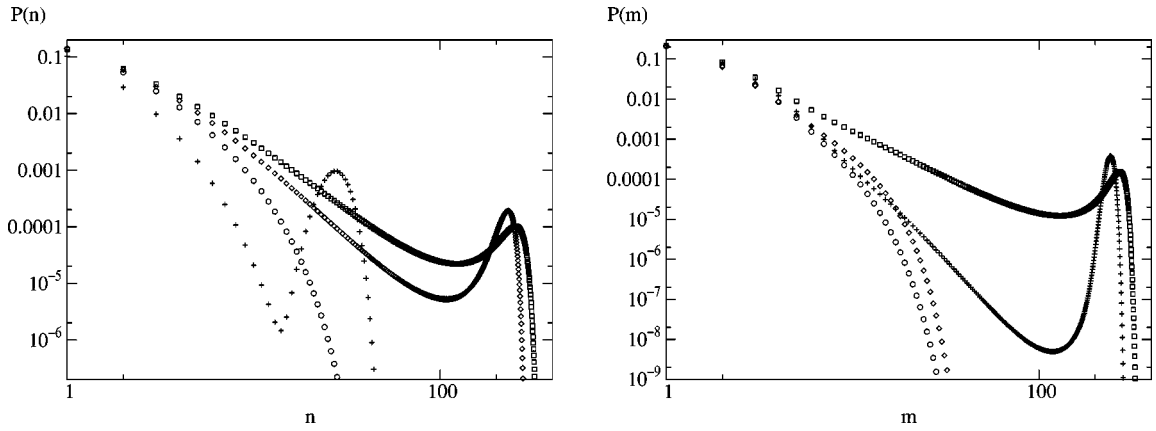

FIG. 6. Log-log plot of on the left $P(n)$ vs n, and on the right $P(m)$ vs m, for systems of size $L=100$ and $b=4$ and $c=2$. The circles correspond to densities $\rho_A=1/2=\rho_B$ (fluid phase); the crosses correspond to densities $\rho_A=1/2$ and $\rho_B=3$ (condensate of B particles is sustained by a "weak" condensate of A particles); the squares correspond to densities $\rho_A=7/2=\rho_B$ (both species condense); the diamonds correspond to densities $\rho_A=3$ and $\rho_B=1/2$ (A particles form a condensate).

$$w(\{\tau_i\}) = \mathrm{Tr}[X_1 \cdots X_{L+N+M}], \tag{27}$$

provided the matrices D, E, and A satisfy the relations

$$\beta DA = A, \tag{28}$$

$$\alpha AE = A, \tag{29}$$

$$DE - qED = D + E. \tag{30}$$

These relations are satisfied if we take A to be the projector $|V\rangle\langle W|$, where we employ a bra-ket notation to denote the left and right vectors $\langle W|$ and $|V\rangle$. With this notation, Eq. (27) becomes

$$w(\{\tau_i\}) = \langle W|X_1 \cdots X_{L+N+M}|V\rangle, \tag{31}$$

and if the lth vacancy is at site k_l, then this can be written as (choosing the normalization $\langle W|V\rangle = 1$ and using the invariance of the trace under cyclic permutations of the X's)

$$w(\{\tau_i\}) = \prod_{l=1}^{L} \langle W|X_{k_l+1} \cdots X_{k_{l+1}-1}|V\rangle, \tag{32}$$

i.e., the steady state weights assume a factorized form—one factor for each vacancy. Now, to make the connection to the two-species zero-range process, we define the matrix $G_{n,m}$ to be the sum over all permutations of products of n D's and m E's. Also, we define $P(\{n_l\};\{m_l\})$ to be the probability that, in between all pairs of vacancies l and $l+1$, there are exactly n_l $+$ particles and m_l $-$ particles. Hence

$$P(\{n_l\};\{m_l\}) = Z_{L,N,M}^{-1} \prod_{l=1}^{L} \langle W|G_{n_l,m_l}|V\rangle, \tag{33}$$

where $Z_{L,N,M}$ is a normalization. Equation (33) is identical to Eq. (1) if we make the identification

$$f(n,m) = \langle W|G_{n,m}|V\rangle, \tag{34}$$

and the normalization $Z_{L,N,M}$ then is given by Eq. (5). This establishes the mapping.

Thus the steady state of the AHR model can be expressed in a form identical to the steady state of the two-species zero-range process if we identify the $+$ particles with the A particles and the $-$ particles with the B particles. The hop rates of the A and B particles, obtained by substituting Eq. (34) into Eq. (2), are given by

$$u(n,m) = \frac{\langle W|G_{n-1,m}|V\rangle}{\langle W|G_{n,m}|V\rangle}$$

and

$$v(n,m) = \frac{\langle W|G_{n,m-1}|V\rangle}{\langle W|G_{n,m}|V\rangle}. \tag{35}$$

Note that because the mapping specifies $f(n,m)$ (and not the hop rates) the hop rates are guaranteed to satisfy the constraint equation (4). Also, this is not a mapping for the dynamics—rather, it is a mapping between steady states which have the same form.

The matrix elements $\langle W|G_{n,m}|V\rangle$ are known exactly [16] and assume different asymptotic forms depending on the values of α, β, and q. Thus the phase behavior of the AHR model is observed in the two-species zero-range process by using these different forms to determine $f(n,m)$ using Eq. (34). We note that the resulting values of the hop rates are different to those studied earlier in this paper: the hop rates as determined via the mapping to the AHR model obey the symmetry $u(n,m) = v(m,n)$ under the interchange $\alpha \leftrightarrow \beta$.

VI. CONCLUSION

We have shown how the steady state of the two-species zero-range process can undergo a number of condensation transitions. A single particle of one species was found to be able to induce condensation in the other above a critical density. Next, for finite densities of both species, we investigated a case where the hop rates of the two species were coupled in a nontrivial way. Three distinct condensate phases emerged and the conditions on the hop rates leading to such phases were presented for quite general rates. This generality suggests that the transition mechanisms are robust.

There remain a number of outstanding questions. A more detailed understanding of the phase where the condensate is sustained by a weak condensate of particles of the other species is desirable. It is also unclear whether there exist further couplings between the particle species which might lead to new transitions. This could require analysis of the model for dynamics which do not satisfy the constraint (4); such investigation may also yield insight into the structure of the steady state when the factorized form does not hold.

ACKNOWLEDGMENTS

T.H. acknowledges EPSRC for financial support under Grant No. GR/52497. We thank D. Mukamel for helpful discussions.

[1] S.N. Majumdar, S. Krishnamurthy, and M. Barma, Phys. Rev. Lett. **81**, 3691 (1998).
[2] P.L. Krapivsky and S. Redner, Phys. Rev. E **54**, 3553 (1996).
[3] M.R. Evans, Europhys. Lett. **36**, 13 (1996).
[4] O.J. O'Loan, M.R. Evans, and M.E. Cates, Phys. Rev. E **58**, 1404 (1998).
[5] P.F. Arndt, T. Heinzel, and V. Rittenberg, J. Phys. A **31**, L45 (1998); J. Stat. Phys. **97**, 1 (1999).
[6] D. Mukamel, in *Soft and Fragile Matter: Nonequilibrium Dynamics, Metastability and Flow*, edited by M. E. Cates and M. R. Evans (Institute of Physics Publishing, Bristol, 2000).
[7] Y. Kafri, E. Levine, D. Mukamel, G.M. Schütz, and J. Török,

Phys. Rev. Lett. **89**, 035702 (2002).
[8] M.R. Evans, Braz. J. Phys. **30**, 42 (2000).
[9] M.R. Evans and T. Hanney, J. Phys. A **36**, L441 (2003).
[10] S. Großkinsky and H. Spohn, Bull. Braz. Math. Soc. N.S. **34**, 1 (2003).
[11] R. Lahiri and S. Ramaswamy, Phys. Rev. Lett. **79**, 1150 (1997).
[12] B. Drossel and M. Kardar, Phys. Rev. Lett. **85**, 614 (2000).
[13] D. Das and M. Barma, Phys. Rev. Lett. **85**, 1602 (2000).
[14] B. Derrida, M.R. Evans, V. Hakim, and V. Pasquier, J. Phys. A **26**, 1493 (1993).
[15] B. Derrida, S.A. Janowsky, J.L. Lebowitz, and E.R. Speer, J. Stat. Phys. **73**, 813 (1993).
[16] K. Mallick, J. Phys. A **29**, 5375 (1996); T. Sasamoto, Phys. Rev. E **61**, 4980 (2000).